

NOISE EFFECTS ON PERFORMANCE OF SIGNAL DETECTION IN AN ANALOG VLSI RESONATE-AND FIRE NEURON

Kazuki Nakada, Jun Igarashi, Tetsuya, Asai, Hatsuo Hayashi*

Kyushu Institute of Technology, Kitakyushu, Fukuoka, 808-0196, Japan

*Hokkaido University, Sapporo, Hokkaido, 060-8628, Japan

ABSTRACT

In this paper, we present analog VLSI implementation of a resonate-and-fire neuron (RFN) model, and then consider noise effects on its performance of signal detection. The RFN circuit is a silicon spiking neuron that has second-order membrane dynamics and exhibits dynamic behavior, such as fast subthreshold oscillation, coincidence detection, frequency preference, and post-inhibitory rebound. Due to such dynamic behavior, the RFN circuit acts as a band-pass filter and a coincidence detector at circuit level. Through SPICE simulations, we will demonstrate noise effects on the coincidence detection and the frequency preference of the RFN circuit.

1. INTRODUCTION

Functional networks of silicon spiking neurons are shown to be useful in a wide variety of applications [3]-[9]. Recent research efforts have concentrated on real-time event-based computation, in which coincidence or synchrony detection plays essential roles in neural information processing, such as auditory perception [6], onset detection [8], and learning and memory [9]-[10]. Temporal filtering properties are also significant to extract temporal structure of spike sequences in which information may be encoded.

Computational performance of such functional networks of silicon spiking neurons are limited if their components are quite simple. For instance, the Axon-Hillock circuit [1], widely known as an electronic analogue of the integrate-and fire neuron (IFN) model, can only act as a low-pass filter. In order to increase their performance, alternative silicon spiking neurons [14]-[21], such as a low-power IFN circuit with frequency adaptation [17] and an asynchronous chaotic spiking neuron circuit [20], have been developed. These circuits increase synchrony detection and temporal filtering properties in network circuits. Synaptic circuits with short-term plasticity can also increase computational performance of silicon spiking neural networks [8], [10]-[13], however, they can only work effectively at network level.

In our previous work, we have proposed analog VLSI implementation of a resonate-and-fire neuron (RFN) model

[22] based on the Volterra system [21]. The RFN model is a spiking neuron model that exhibits dynamic behavior observed in biological neurons, such as fast subthreshold oscillation, coincidence detection, post-inhibitory rebound, and frequency preference. Due to such dynamic behavior, the RFN circuit acts as a coincidence detector and a band-pass filter at circuit level, and thus it is expected to be useful for large-scale implementation of functional silicon spiking neural networks.

In the present work, we consider noise effects on the performance of the signal detection in the RFN circuit. By using SPICE, we will show that random pulses modulate the frequency preference to inputs, and then the circuit has the noise robustness of the coincidence detection. These results imply that the RFN circuit can work effectively and efficiently under practical conditions, and provide us with guidelines for implementing it into silicon chips.

2. ANALOG VLSI RESONATE-AND-FIRE NEURON

We here describe analog VLSI implementation of a resonate-and-fire neuron (RFN) model.

2.1. Resonate-and-Fire Neuron Model

The RFN model is a spiking neuron model proposed by Izhikevich, which has second-order subthreshold membrane dynamics and a firing threshold [22]. The dynamics of the RFN model are described by:

$$\dot{x} = bx - wy + I \quad (1)$$

$$\dot{y} = wx + by \quad (2)$$

or by an equivalent complex form:

$$\dot{z} = (b + iw)z + I \quad (3)$$

where $z=x+iy$ is a complex variable, the real and imaginary parts, x and y , are the current- and voltage-like variables, respectively, b and w are parameters, and I is an external input. If $\text{Im } z$ exceeds a certain threshold a_{th} , z is reset

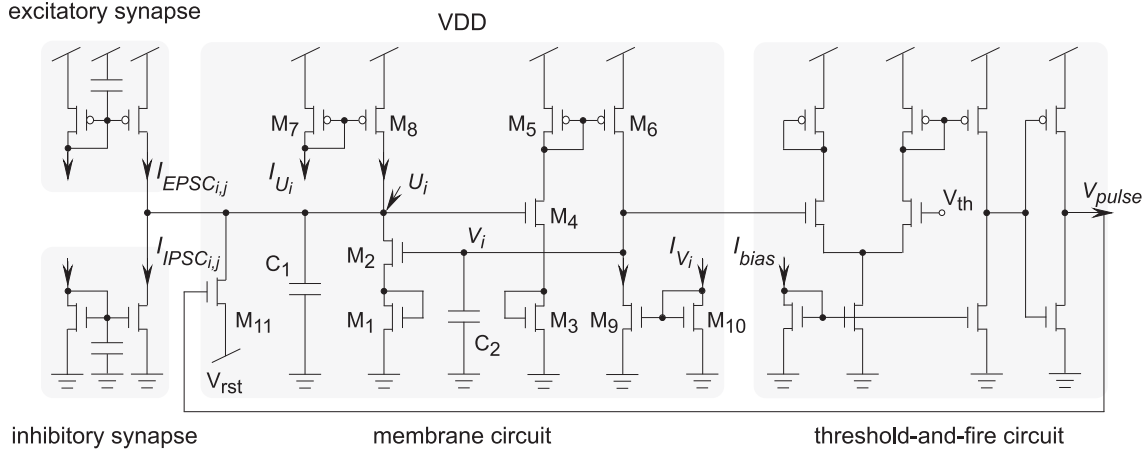


Fig. 1. Schematic of the resonate-and-fire neuron circuit. The circuit consists of a membrane circuit, a threshold-and-fire circuit, and excitatory and inhibitory synaptic circuits. The membrane circuit has second-order dynamics and two state variables U_i and V_i , and thus shows oscillatory behavior. Synaptic inputs change the trajectory of the oscillation, and if V_i exceeds a threshold voltage V_{th} , the threshold-and-fire circuit generates a spike V_{pulse} and resets U_i to a bias voltage V_{rst} .

to an arbitrary value z_o , which describes activity-dependent after-spike reset. This model has second-order membrane dynamics, and thus exhibits dynamic behavior, such as fast subthreshold oscillation, resulting in coincidence detection, post-inhibitory-rebound, and frequency preference [22].

2.2. Circuit Implementation

We designed the RFN model as an analog integrated circuit in the previous work [21]. Figure 1 shows the schematic of the RFN circuit, which consists of a membrane circuit, a threshold-and-fire circuit, and current mirror integrators as excitatory and inhibitory synaptic circuits [2].

The membrane circuit was derived from the Volterra system for modeling prey-predator interactions to mimic membrane dynamics of the RFN model by using the current-voltage relationship of subthreshold MOS FETs [21]. The dynamics of the membrane circuit are described as follows:

$$C_1 \frac{dU_i}{dt} = -g(U_i - V_{rst}) + I_{in} + \bar{I}_{U_i} - I_o \exp\left(\frac{\kappa^2}{\kappa + 1} \frac{V_i}{V_T}\right) \quad (4)$$

$$C_2 \frac{dV_i}{dt} = I_o \exp\left(\frac{\kappa^2}{\kappa + 1} \frac{U_i}{V_T}\right) - \bar{I}_{V_i} \quad (5)$$

where voltages U_i and V_i are state variables, C_1 and C_2 the capacitances, g the leak conductance of the transistor M_{11} , κ the capacitive coupling ratio from the gate to the channel, V_T the thermal voltage, and I_o the pre-exponential current [2]. I_{in} represents a summation of synaptic currents:

$$I_{in} = \sum_j I_{EPSC_{i,j}} - \sum_j I_{IPSC_{i,j}} \quad (6)$$

where $I_{EPSC_{i,j}}$ and $I_{IPSC_{i,j}}$ represent the i -th post-synaptic currents through the j -th excitatory and inhibitory synaptic

circuits. Currents, \bar{I}_{U_i} through M_8 and \bar{I}_{V_i} through M_9 , are approximately described as follows:

$$\bar{I}_{U_i} = \alpha I_{U_i} \left(1 + \frac{VDD - U_i}{V_{E,p}}\right) \quad (7)$$

$$\bar{I}_{V_i} = \beta I_{V_i} \left(1 + \frac{V_i}{V_{E,n}}\right) \quad (8)$$

where I_{U_i} and I_{V_i} are bias currents, VDD the power-supply voltage, $V_{E,p}$ and $V_{E,n}$ the Early voltage [2] for an nMOS FET and a pMOS FET, respectively, and α and β the fitting constants.

The equilibrium point of the circuit, (U_o, V_o) , can easily be calculated, and the stability of the point can be analyzed by the eigenvalues of the Jacobian matrix of the circuit,

$$J = \begin{bmatrix} -\frac{\alpha I_{U_i}}{V_{E,p}} & -\frac{\kappa^2}{\kappa+1} \frac{I_{V_o}}{V_T} \\ \frac{\kappa^2}{\kappa+1} \frac{I_{U_o}}{V_T} & -\frac{\beta I_{V_i}}{V_{E,n}} \end{bmatrix} \quad (9)$$

where I_{U_o} and I_{V_o} represent the equilibrium currents at the equilibrium point, and we assumed the leak conductance g is zero. We used diode-connected transistors for M_1 - M_4 and short transistors that have small Early voltages for M_7 - M_{10} . As a result, the equilibrium point became a focus, and thus the membrane circuit exhibited damped oscillation in response to an input. In this case, the circuit dynamics is equivalent to the membrane dynamics of the RFN model near the equilibrium point.

Inputs thorough synaptic circuits change the trajectory of the oscillation of the membrane circuit. If V_i exceeds a threshold voltage V_{th} , the threshold-and-fire circuit that consists of a comparator and an inverter generates a spike (a pulse voltage V_{pulse}) and resets U_i to a bias voltage V_{rst} . Thus, the behavior of the RFN circuit is qualitatively the same as that of the RFN model.

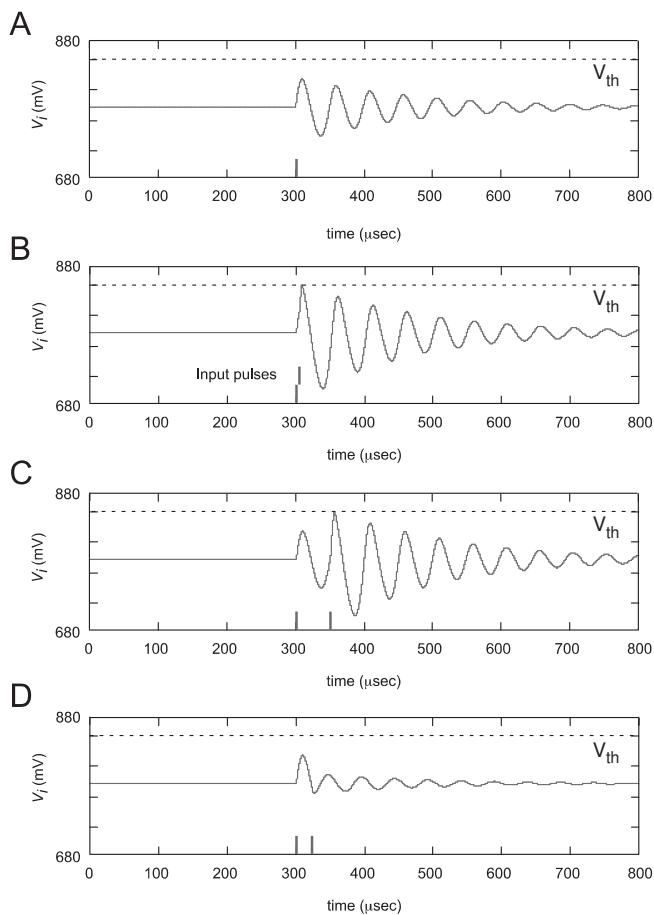


Fig. 2. Typical behavior of the RFN circuit.

3. RESULTS

We here show the performance of the signal detection in the RFN circuit using the circuit simulator, T-Spice Pro, with the model parameters for the AMI 0.35- μm CMOS process.

In the following simulations, the supply voltages were set at $V_{DD}=1.5\text{ V}$, $V_{th}=830\text{ mV}$, and $V_{rst}=750\text{ mV}$, the bias current were set at $I_{U_i}=I_{V_i}=10\text{ nA}$, and $I_{bias}=250\text{ nA}$, and the capacitance were set at $C_1=C_2=1.2\text{ pF}$. We used pulse currents (width: $1\ \mu\text{sec}$) as synaptic inputs.

Figures 2 show typical behavior of the RFN circuit in response to synaptic inputs. When a weak pulse (EPSC) that cannot evoke a action potential (amplitude: 55 nA) arrives at the circuit, a damped subthreshold oscillation occurs, as shown in Fig. 2A. When two pulses (EPSCs) arrive at the circuit at an interval of about $5\ \mu\text{s}$ (Fig. 2B) or the interval between the two pulses is nearly equal to the period of the oscillation, $50\ \mu\text{s}$ (Fig. 2C), the circuit fires a spike. The RFN circuit, however, does not fire a spike when the interval between the two pulses is in other ranges (Fig. 2D). These results indicate that the circuit is resonant with a sequence of pulses at a resonance frequency, i.e., frequency preference, and thus the circuit acts as a band-pass filter.

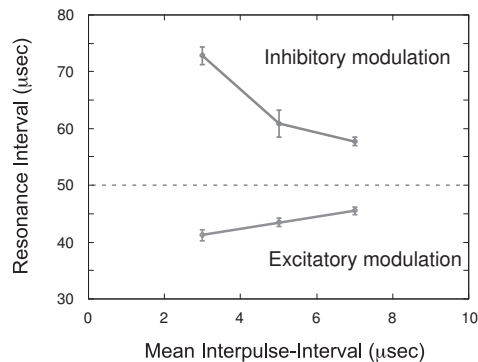


Fig. 3. Frequency preference modulation.

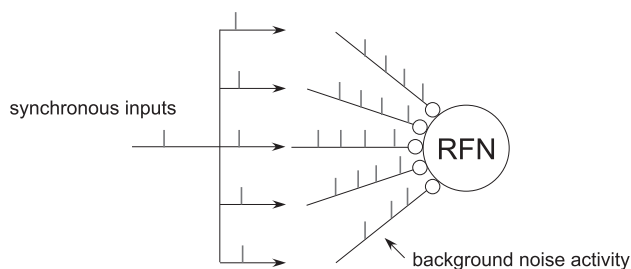


Fig. 4. Network for coincidence detection.

We here show how random pulses affects the frequency preference in the RFN circuit. We employed a sequence of random pulses as background activity. The inter-pulse-interval (IPI) of the pulses were generated by the Gaussian distribution (the ratio of the standard deviation to the mean IPI: 0.1). We set the amplitude of the pulses at 20 nA for excitation and -20 nA for inhibition, respectively. Figure 3 shows the relationships between the resonance interval of the circuit and the mean IPI of the background noises. These relationships indicate that the frequency preference of the circuit are modulated by the background noisy activity.

We then show the noise robustness of the coincidence detection in the RFN circuit. We consider an RFN circuit with five excitatory synaptic circuits, each of which carries background random pulses (the mean of IPI: $7\ \mu\text{sec}$) and rarely synchronous signals to the RFN circuit, as shown in Fig. 4. The RFN circuit can detect synchronous signals embedded in background pulses. If the frequency of the background noisy pulses is high, these pulses are filtered by the band-pass characteristics of the RFN circuit and the synchronous signals can be detected at the same time since the RFN circuit acts as a coincidence detector. In contrast, many IFN circuits fire a spike in response to background noises. Figure 5 shows that the coincidence detection of synchronous signals given from $300\ \mu\text{sec}$ to $302\ \mu\text{sec}$ in the presence of background noisy activity.

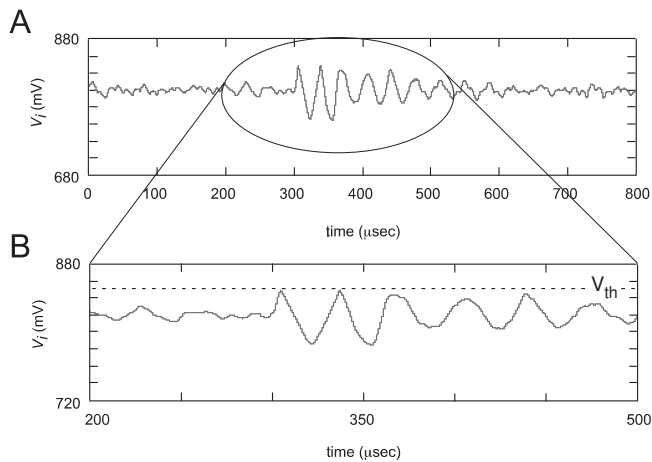


Fig. 5. Noise robustness of coincidence detection.

4. CONCLUSIONS

We have shown the performance of the signal detection in the RFN circuit. First, we have considered how random noisy inputs modulate the resonance interval of the RFN circuit. We have also shown that the RFN circuit can detect synchronous signals embedded in background noises since the RFN circuit act as a band-pass filter and a coincidence detector at the same time. These results imply that the RFN circuit work effectively in the presence of background noisy activity and to be useful for practical applications.

5. REFERENCES

- [1] C. A. Mead, *Analog VLSI and neural systems*, Addison-Wesley, Reading, 1989.
- [2] S.-C. Liu, J. Kramer, G. Indiveri, T. Delbruck, and R. Douglas, *Analog VLSI: Circuits and Principles*, MIT Press, 2002.
- [3] S.-C. Liu, J. Kramer, G. Indiveri, T. Delbruck, T. Burg, and R. J. Douglas, "Orientation-selective aVLSI spiking neurons," *Neural Networks*, vol. 14, no. 6-7, pp. 629-643, 2001.
- [4] F. Tenore, R. Etienne-Cummings, and M. A. Lewis, "A programmable array of silicon neurons for the control of legged locomotion," in *proc. IEEE Int. Symp. Circ. Syst.*, 2003.
- [5] E. Culurciello, R. Etienne-Cummings, and K. Boahen, "A biomorphic digital image sensor," *IEEE Journal of Solid-State Circuits*, vol. 8 no. 2, pp. 281 -294, 2003.
- [6] M. Cheely and T. Horiuchi, "Analog VLSI models of range-tuned neurons in the bat echolocation system," *EURASIP J. Appl. Signal Proc.*, vol. 7, pp. 649-658, 2003.
- [7] S.-C. Liu and R. J. Douglas, "Temporal coding in a network of silicon integrate-and-fire neurons," *IEEE Trans. Neural Networks*, Vol. 15, NO.5, pp. 1305-1314, 2004.
- [8] Y. Kanazawa, T. Asai, M. Ikebe, and Y. Amemiya, "A novel CMOS circuit for depressing synapse and its application to contrast-invariant pattern classification and synchrony detection," *Int. J. Robotics and Automation*, vol. 19, no. 4, pp. 206-212, 2004.
- [9] H. Tanaka, T. Morie, K. Aihara, "Associative memory operation in a Hopfield-type spiking neural network with modulation of resting membrane potential," presented at *Int. Symp. on Nonlinear Theory and its Applications*, Bruges, Belgium, 2005.
- [10] G. Indiveri, E. Chicca and R. J. Douglas, "A VLSI array of low-power spiking neurons and bistable synapse with spike-timing dependent plasticity," *IEEE Trans. Neural Networks*, to be appeared.
- [11] C. Rasche and R. H. R. Hahnloser, "Silicon synaptic depression," *Biol. Cybern.*, vol. 84, pp. 57-62, 2001.
- [12] S.-C. Liu, "Analog VLSI circuits for short-term dynamic synapses," *EURASIP J. Appl. Signal Proc.*, vol. 7, pp 620-628, 2003.
- [13] A. Bofill-i-Petit and A. F. Murray, "Synchrony detection and amplification by silicon neurons With STDP synapses," *IEEE Trans. Neural Networks*, Vol. 15, NO.5, pp. 1296- 1304, 2004.
- [14] S. R. Schultz and M. A. Jabri, "Analogue VLSI integrate-and-fire neuron with frequency adaptation," *Electronic Letters*, vol. 31, no. 16, pp. 1357-1358, 1995.
- [15] K. A. Boahen, *Retinomorph VIPLon Systems: Reverse Engineering the Vertebrate Retina*, Ph.D. thesis, California Institute of Technology, Pasadena CA, 1997.
- [16] A. van Schaik, "Building blocks for electronic spiking neural networks," *Neural Networks*, vol. 14, no. 6-7, pp. 617-628, 2001.
- [17] G. Indiveri, "A low-power adaptive integrate-and-fire neuron circuit," in *proc. IEEE Int. Symp. Circ. Syst.*, 2003.
- [18] T. Asai, Y. Kanazawa, and Y. Amemiya, "A subthreshold MOS neuron circuit based on the Volterra system," *IEEE Trans. Neural Networks*, vol. 14, no. 5, pp. 1308-1312, 2003.
- [19] H. Nakano and T. Saito, "Grouping synchronization in a pulse-coupled network of chaotic spiking oscillators," *IEEE Trans. Neural Networks*, vol. 15, no. 5, pp. 1018-1026, 2004.
- [20] Y. Horio, T. Taniguchi and K. Aihara, "An Asynchronous Spiking Chaotic Neuron Integrated Circuit," *Neurocomputing*, Vol. 64, pp. 447-472, 2005.
- [21] K. Nakada, T. Asai, H. Hayashi, "A silicon resonate-and-fire neuron on the Volterra system," presented at *Int. Symp. on Nonlinear Theory and its Applications*, Bruges, Belgium, 2005.
- [22] E. M. Izhikevich, "Resonate-and-fire neurons," *Neural Networks*, vol. 14, pp. 883-894, 2001.